Microstructure of Hardened Steel at High Temperature and High Strain Rate

Ding Feng, *Tang Dewen*, *Wang Chengyong* *, *Zhang Fenglin*, *Zheng Lijuan*

Guangdong University of Technology, Guangzhou, 510006, P. R. China

(Received 29 September 2015; revised 7 March 2016; accepted 12 March 2016)

Abstract: In high-speed machining, hardened steel materials are subjected to high temperatures and high strain rates. Under these conditions, the composition and microstructure of the material may change, and phenomena, such as thermal softening, emerge. These effects are difficult to detect by only observing the chip morphology. Here, using a microscopic detection method, the dynamic mechanical behavior and microstructure of SDK11 hardened steel (62 HRC) is investigated at high temperature and high strain-rate, and the relationship between strain hardening, thermal softening, and strain-rate strengthening is determined. The metallographic phases of specimens treated using a split-Hopkinson pressure bar, and "chips" generated during high-speed machining at high temperature and high strain rate state are compared. The results indicate that the phase composition at low temperature and low strain rate differs from that at high temperature and high strain rate. It is further concluded that shear slip occurs at high temperature and high strain rate, and the shear behavior is more pronounced at higher strain rates.

Key words: microstructure; microscopic detection method; hardened steel; split-Hopkinson pressure bar

CLC number: TG115 **Document code**: A **Article ID**: 1005-1120(2017)04-0380-08

0 Introduction

Hardened steel (52-62 HRC) exhibits typical high-temperature characteristics and high strain rates (10^4—10^6 s)[1-2] in high-speed cutting processes. The split-Hopkinson pressure bar (SHPB) is widely used to investigate the dynamic mechanical properties of materials at high temperature and high strain rate to simulate the formation of materials during high-speed machining[3]. In this method, however, the strain of instantaneous shock compression is small and the strain rates generated are smaller than those attained during high-speed cutting[4]. Nevertheless, the SHPB has advantages in terms of studying the interaction of parameters, such as stress, strain, strain rate, and temperature.

Based on SHPB experiments, Fu et al.[5] investigated the relationship among strain, strain rate and flow stress for aluminum alloy 7050-T7451 from room temperature to 550 °C, and determined flow stress constitutive model based on Johnson-Cook empirical model (J-C model). Zhang et al.[6] researched the dynamic mechanism behavior of aluminum alloy 2A70, and introduced the standard Johnson-Cook strain rate term and several derivative forms and calibrated by the test data. Seo et al.[7] studied the effect of temperature on strain and strain rate for Ti-6Al-4V, observed the thermal gradients in the specimens, and determined a modified J-C model. Xiong et al.[8] investigated the effect of temperature on microstructure and deformation mechanism of Fe-30Mn-3Si-4Al twinning-induced plasticity steel, found the interaction among flow stress, density and temperatures, and calculated stack fault energy using thermodynamic data. Zhang et al.[9] tested the dynamic response of Q345 steel under extreme loading conditions of high temperatures

* Corresponding author: E-mail: cywang@gdut.edu.cn.

How to cite this article: Ding Feng, Tang Dewen, Wang Chengyong, et al. Microstructure of hardened steel at high temperature and high strain rate[J]. Trans. Nanjing Univ. Aero. Astro., 2017,34(4):380-387.
http://dx.doi.org/10.16356/j.1005-1120.2017.04.380

and dynamic shock load, obtained the stress-strain curve of Q345 steel impacted on different shock times, and figured out the relationship between strength and strain rate is nonlinear.

At present, there are few studies on the dynamic behavior of high-hardness steel at high temperature and high strain rate. Our group[10] previously investigated the dynamic mechanical properties of SKD11 (62 HRC) based on SHPB experiment, obtained stress-strain curves and a constitutive equation of the steel at high temperature and high strain rates, and analyzed the changes in the stress-strain curves from a macroscopic perspective. However, the cause of the changes in the stress-strain curves could not be accurately explained in terms of a macroscopic perspective. Therefore, in the present study, we analyzed the microstructure of hardened steel at high temperature and high strain rates using X-ray diffraction (XRD) and scanning electron microscopy (SEM), and explained, from a microscopic viewpoint, the stress-strain relationship reported in previous study[10]. Moreover, we compare the material morphology determined using SHPB with the morphology of chips formed during high-speed cutting. The results of this study shed light on chip formation in the high-speed cutting of hardened steel.

1 Materials and Methods

1.1 Materials

The material investigated was cold-work die steel SKD11, which is used in high-speed cutting processes. The chemical composition and hardness are shown in Table 1. SKD11 specimens were quenched at 980—1 020 °C and tempered twice at 180—200 °C to achieve a hardness of 60 HRC. The microstructure of SKD11 after being quenched is shown in Fig. 1(a), in which the organization of many fine particles into a sheet can be observed. Moreover, a high fraction of Cr in the carbide particle surface was revealed by energy dispersive spectrometer (EDS) analysis.

Table 1 Chemical composition of SKD11 %

C	Cr	Mo	Si	Mn	V
1.4—1.6	11.0—13.0	0.7—1.2	≤0.6	≤0.6	0.15—0.3

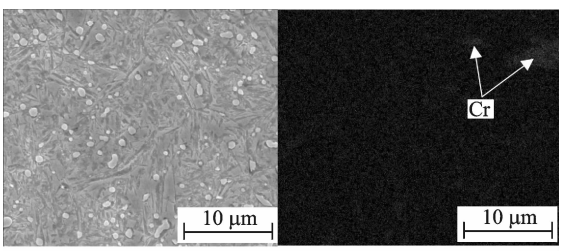

Fig. 1 Microstructure of SKD11 (62 HRC)[11]

1.2 Methods

A sketch of the SHPB is shown in Fig. 2. During the experiment, the bullet with a certain speed hits the input bar. The foil gauges in the input and transmission bars record the transmitted signal, which is used to determine the input signal. Based on the one-dimensional stress-wave principle[12], the relationship between the stress, strain, and strain rate can be obtained.

The SHPB was used to obtain the dynamic mechanical properties of SKD11 at temperatures of 20, 300, 600, and 800 °C, and strain rates of 0.01, 500, 5 000, and 10 000 s^{-1}. The specimens were ground, polished, and etched after the experiment, then analyzed using XRD and SEM.

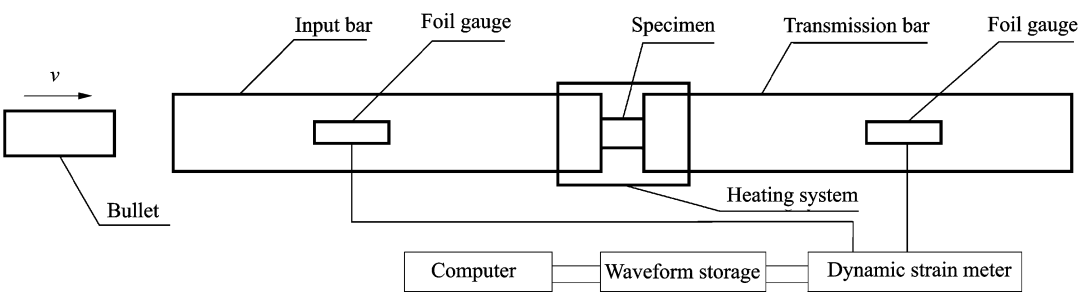

Fig. 2 Sketch of the split-Hopkinson pressure bar[13]

2 Results and Discussions

The shape changes of the specimens at different temperatures and strain rates after the SHPB experiments are shown in Fig. 3. The length change is shown in Fig. 4 as a function of deformation temperature. These results show that material exhibits dynamic thermal softening with increasing temperature and that this is most significant above 300 ℃. Moreover, significant shear slip is generated in the specimens at strain rates of $5 \times 10^2\ s^{-1}$ or higher. The dynamic softening and deformation are greater at higher temperatures and higher strain rates.

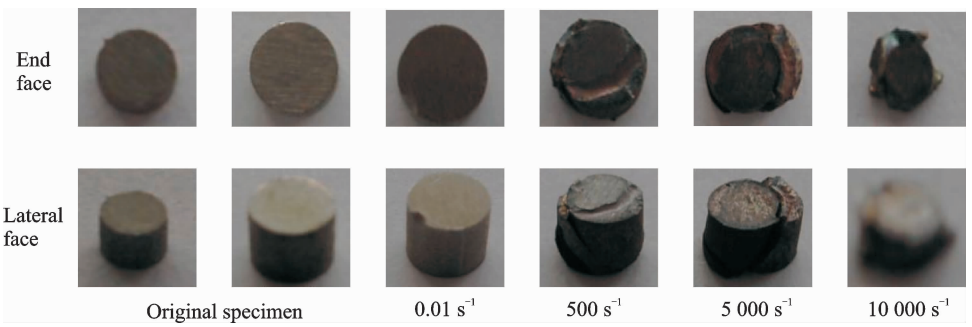

Fig. 3 Photographs of the original specimen and those deformed at 600 ℃ with different strain rates

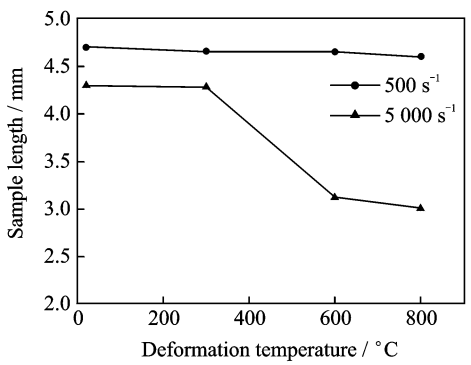

Fig. 4 Compression deformation of the specimen at strain rates of 500 and 5 000 s^{-1}

The stress-strain curves of the specimens treated using the SHPB are shown in Fig. 5. In the initial stages of compression, the flow stress increases rapidly with the increasing strain. After reaching a critical value, the rate of increase in flow stress decreases significantly. When the flowstress reaches the end of compression deformation, it decreases sharply. At different temperatures, the stress-strain curves show different degrees of microwave phenomenon. With increasing temperature and strain rate, the wave becomes more pronounced , which is the result of

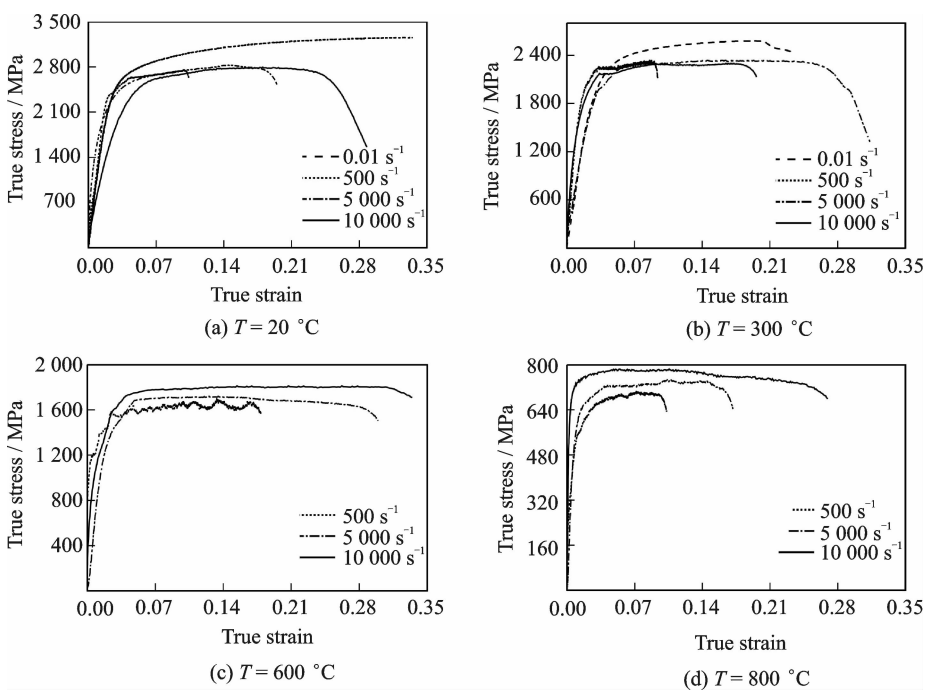

Fig. 5 Stress-strain curves of hardened steel SKD11 at different temperatures

dynamic softening of the hardened steel.

It also can be seen from Fig. 5(a) that at 20 °C, the flow stress increases and significant strain hardening occurs during the initial stages of compression. Beyond the yield stage, the curves are flat with respect to the strain axis, which is close to ideal plastic behavior[14]. At high temperature, the increased stress limits the increase of strain. However, the flow stress slightly decreased with increasing strain at temperatures below 600 °C, which reflects the negative strain effect of materials at low temperature. In addition, with increasing temperature and strain rate, the stress decreases owing to the thermal softening effect.

2.1 Effect of temperature on microstructure

To analyze the effect of temperature on the microstructure of SKD11, the specimens were analyzed using XRD; the results are shown in Fig. 6. The primary surface phases of SKD11 at temperatures in the range of 20—800 °C include FeCr and FeCrC alloys. At 20 °C, owing to the higher strain rate, the instantaneous strain was higher and elemental α-Fe was generated when the strain energy exceeded the FeCr alloy bond energy, as shown in Fig. 6(a). At 600 °C, because of the high strain rate and temperature, the strain energy of the high-speed impact resulted in breaking of the FeCr alloy bond break, which released elemental α-Fe. However, at high temperature, newly formed elemental Fe quickly oxidized. Therefore, new Fe_2O_3 and $FeCrO_4$ phases were generated on the surface of the hardened steel.

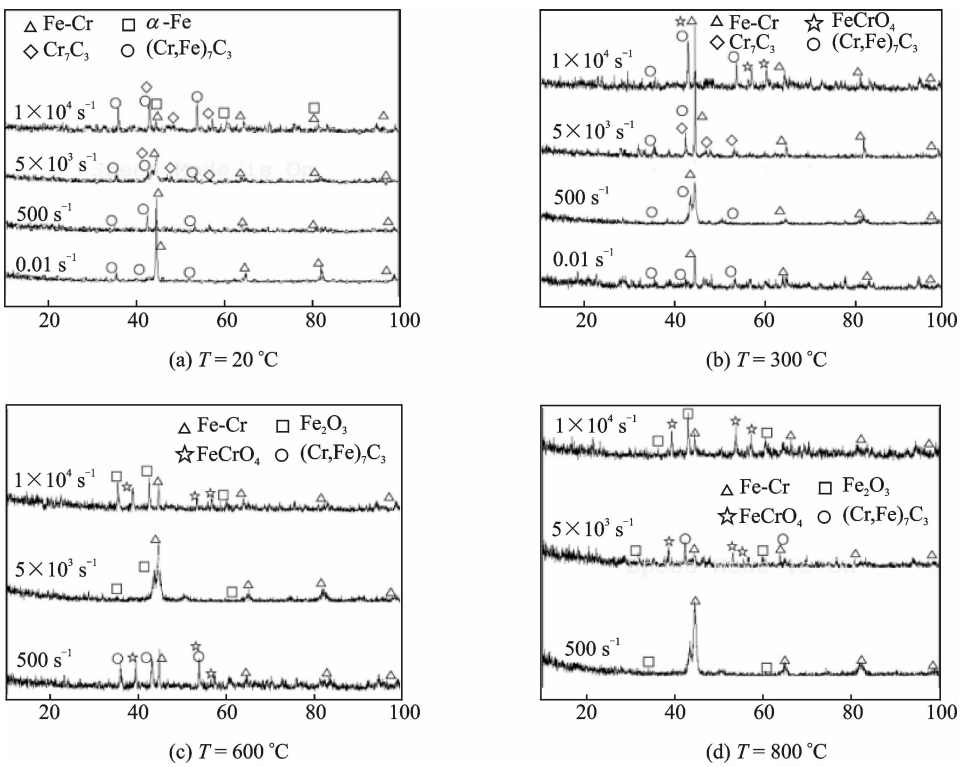

Fig. 6 XRD patterns of SKD11 hardened steel surfaces treated at different temperatures

SEM was used to analyze the surfaces of the specimens; the results are shown in Figs. 7—10. The surfaces of brittle fracture specimens treated at 20 and 300 °C are covered with tiny microcracks. This demonstrates that cracks are generated inside the material and rapidly expand during loading. However, since the plastic deformation capacity of the material is low during loading, damage occurs when the material is deformed slightly. Material strain softening behavior caused by cracking was observed, as shown in Figs. 7, 8, which reflects the negative strain-rate effect. Crack propagation is restricted by plastic deformation. With increasing temperature, the plastic deformation capacity of a material at high strain rate increases; thus, the higher the tem-

perature, the greater the extent to which plastic deformation is impeded, and the more obvious the strain softening behavior becomes. Therefore, during high-strain-rate experiments and low temperatures, the specimen fractures into two halves after slight strain softening, whereas at higher temperatures, owing to the strong plastic deformation capacity (which results in crack formation and expansion), strain softening behavior occurs, as shown in Figs. 9,10.

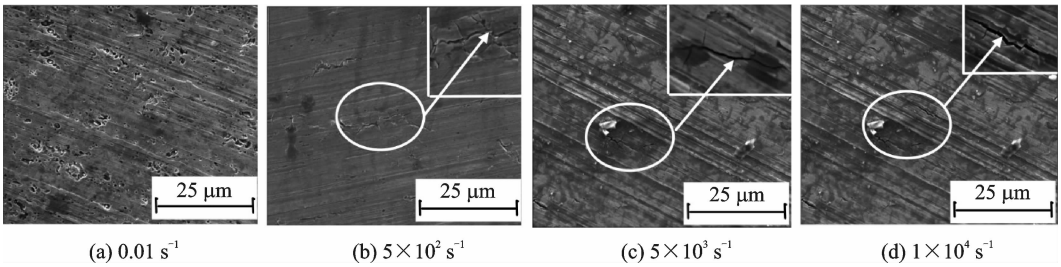

Fig. 7 Surface morphology of SKD11 hardened steel treated at 20 °C

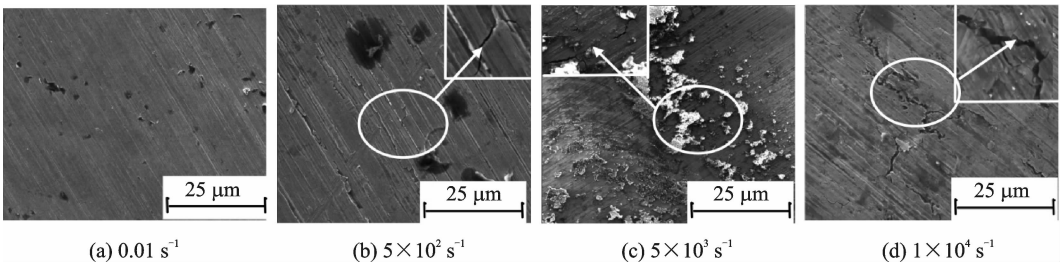

Fig. 8 Surface morphology of SKD11 hardened steel treated at 300 °C

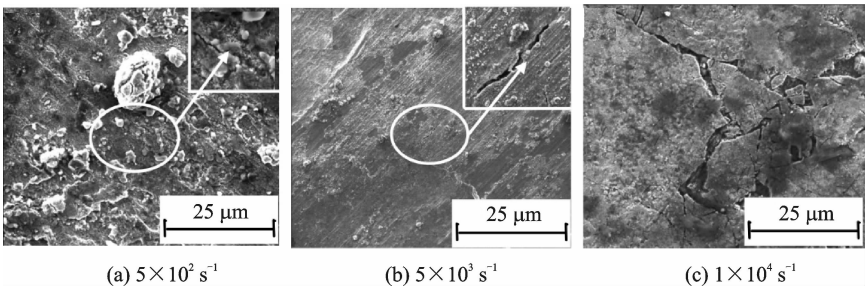

Fig. 9 Surface morphology of SKD11 hardened steel treated at 600 °C

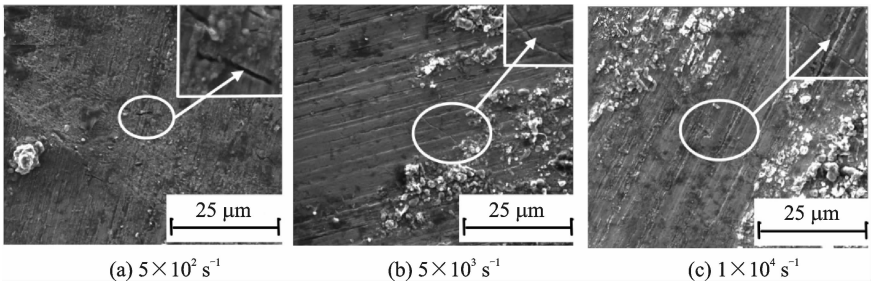

Fig. 10 Surface morphology of SKD11 hardened steel treated at 800 °C

2.2 Effect of strain rate on microstructure

In Fig. 11, the FeCrC alloy grain organization and microstructures of hardened steel treated are shown with different strain rates at 20 °C. At a strain rate of 0.01 s^{-1} (Fig. 11(a)), the alloy grains are approximately the same size as those in the original specimen; however, there are many microcracks on the surface of the carbide particles. At higher strain rates of 5×10^{2} s^{-1} and 5×10^{3} s^{-1} (Figs. 11(b,c)), microcracks can still be observed and the grain size is significantly larger. When the strain rate was increased to 1×10^{4} s^{-1}, the size of the grain alloy was significantly reduced, but no cracks were apparent. With in-

creasing strain rate, the specimens underwent significant shear slip (from macrographic observation; right corner in Fig. 11) and increased in hardness, as shown in Fig. 12.

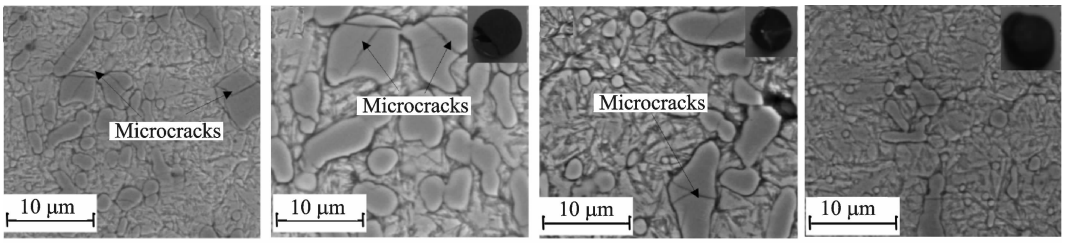

Fig. 11 Microstructure of FeCrC treated at 20 °C

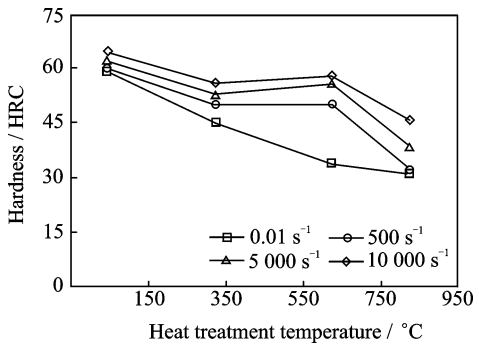

Fig. 12 Hardness of hardened steel as a function of temperature at different strain rates

The FeCrC alloy grain organization and microstructures are shown in Fig. 13 for hardened steel treated at different strain rates at 300 °C. Compared with the case at 20 °C shown in Fig. 11, at a given strain rate, the grain size is larger. Moreover, the grain size increased with strain rate, and microcracks appeared at low strain rate (0.01 and 5×10^{2} s^{-1}); at higher strain rates, the grains appeared significantly refined and no microcracks were present. From analysis of the macrographic images (Fig. 13), specimens were observed to undergo significant shear slip. In contrast to the behavior observed at 20 °C, the hardness significantly reduced because of the high-temperature thermal softening effect, as shown in Fig. 12.

The FeCrC alloy grain organization and microstructures are shown in Fig. 14 for hardened steel treated at different strain rates at 600 °C. Compared with the behavior at 20 and 300 °C, at a given strain rate, the grain structure was significantly coarser. With increasing strain rate, coarseness increased. At a strain rate of 5×10^{2} s^{-1}, significant slippage occured on the surface of the carbide, and at 1×10^{4} s^{-1}, the grains were refined with no obvious microcracks on the surface. From analysis of the macrographic images (Fig. 14), the specimens were found to exhibit shear behavior. At higher strain rates, as the strain-rate-hardening effect exceeded thermal softening effect, the hardness did not decrease but increased, as shown in Fig. 12.

The FeCrC alloy grain organization and microstructures are shown in Fig. 15 for hardened steel treated with different strain rates at 800 °C. In this case, at a given strain rate, the change in grain structure was similar to that observed at 600 °C. At a strain rate of 5×10^{2} s^{-1}, significant slippage occured on the surface and obvious microcracks appeared. From macrographic analysis (Fig. 15), the specimens were observed to first increase in thickness before shear slip occurred. In this case, the hardness of the material was low, which resulted from the thermal-softening effect being dominant, compared with the strain rate hardening effect.

At 800 °C and a strain rate of 10^{4} s^{-1}, microcracks formed and the grain size was small, as shown in Fig. 16(a). Compared with the morphology of the chips formed in the cutting process at 300 m/min (Fig. 16(b)[15]), the metallographic phase of the specimen treated using SHPB (Fig. 16(a)) was more compact, which was the result of the higher strain rate in the shear zone in high-speed cutting than that in the SHPB experiment. This shows that the shear behavior of hardened steel is more pronounced at higher strain rates.

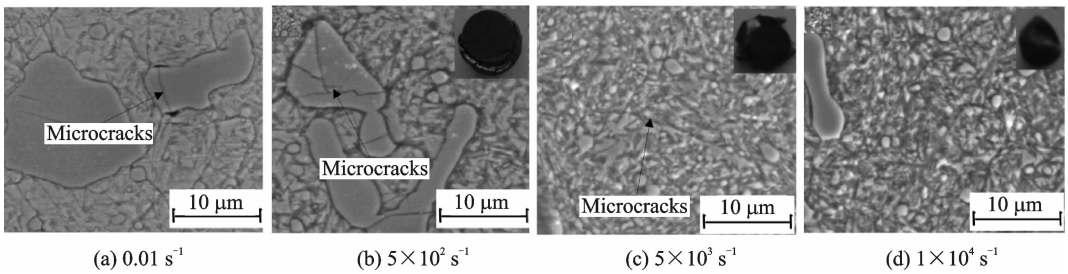

Fig. 13 Microstructure of FeCrC treated at 300 °C

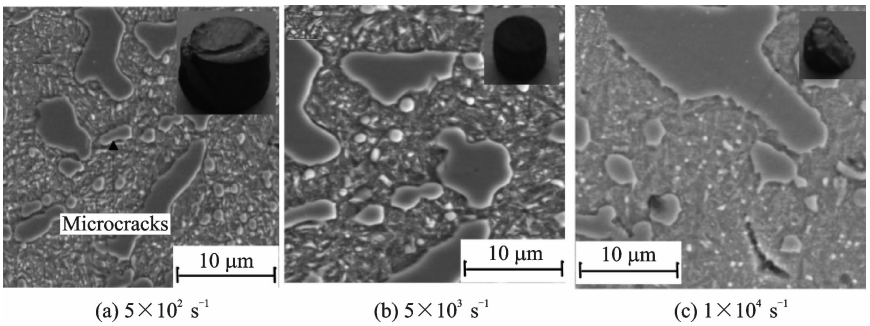

Fig. 14 Microstructure of FeCrC treated at 600 °C

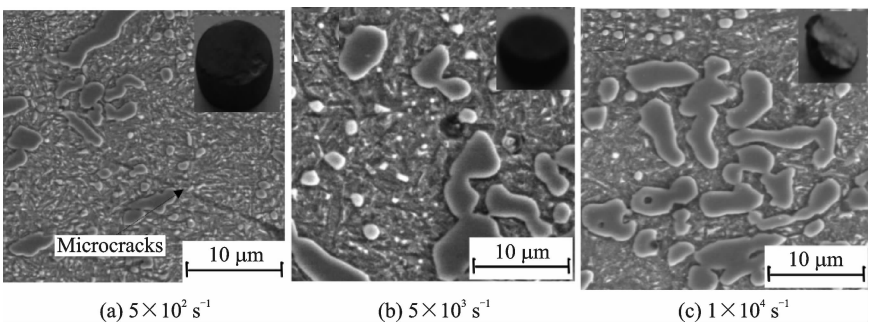

Fig. 15 Microstructure of FeCrC treated at 800 °C

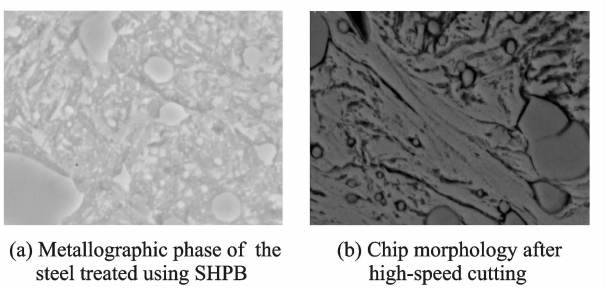

Fig. 16 Metallographic phase of the steel treated using SHPB and chip morphology after high-speed cutting[15] (parameters used were: (a) Strain rate= 10^4 s^{-1}, T= 800 °C; (b) v =300 m/min, α =5°, μ= 0.65, a_e= 4 mm, and a_p= 0.3 mm)

3 Conclusions

With increasing temperature and strain rate, the alloy particle size in SKD11 specimens was found to initially increase and then decrease; whereas for the hardness, the opposite trend was observed. When the specimen was subjected to low temperatures and strain rates, the surface phases mainly included FeCr alloy, Cr_7C_3, and Fe. Moreover, under these conditions, many surface microcracks were observed, resulting from brittle fracture. However, at high temperature and strain rate, the surface phases mainly included FeCr alloy, $FeCrO_4$, and Fe_2O_3. Furthermore, under these conditions, obvious shear slip behavior was found in the core of the specimen and no microcracks were observed on the surface. The hardened steel materials in this study exhibited significant strain hardening, strain-rate hardening and high-temperature softening, and a negative strain-rate effect during the high-speed impact process. Comparison of the metallographic

phase of the specimen treated using SHPB with the morphology of chips formed during cutting revealed that the shear behavior of hardened steel was more pronounced at higher strain rates.

Acknowledgment

The authors gratefully acknowledge the Key Program of the NSFC-Guangdong Joint Fund, China (No. U1201245).

References:

[1] LEI S, SHIN Y C, INCROPERA F P. Material constitutive modeling under high strain rates and temperatures orthogonal machining tests [J]. Journal of Manufacturing Science and Engineering, 1999, 121: 577-584.

[2] SHATLA M, KERK C, ALTAN T. Process modeling in machining (Part I): Determination of flow stress data [J]. International Journal of Machine Tool and Manufacture, 2001, 41: 1511-1534.

[3] KOSHY P, DEWES R C, ASPINWALL DK. High speed end milling of hardened AISI D2 tool steel (58 HRC) [J]. Journal of Materials Processing Technology, 2002, 127: 266-273.

[4] LIU Z Q, WU J H. SHI Z Y, et al. State-of-the-art of constitutive equations in metal cutting operations [J]. Tool Engineering, 2008, 42(3): 3-9. (in Chinese)

[5] FU X L, AI X, WAN Y, ZHANG S. Flow stress modeling for aeronautical aluminum alloy 7050-T7451 in high-speed cutting [J]. Transactions of Nanjing University of Aeronautics & Astronautics, 2007, 24 (2): 139-144.

[6] ZHANG T, CHEN W, GUAN Y P. Dynamic mechanism behavior and constitutive relations of aluminum alloy 2A70 [J]. Journal of Nanjing University of Aeronautics & Astronautics, 2013, 45(3): 367-372. (in Chinese)

[7] SEO S, MIN O, Yang H. Constitutive equation for Ti-6Al-4V at high temperatures measured using the SHPB technique [J]. International Journal of Impact Engineering, 2005, 31:735-754.

[8] XIONG Z P, REN X P, SHU J, et al. Effect of temperature on microstructure and deformation mechanism of Fe-30Mn-3Si-4Al TWIP steel at strain rate of 700 s^{-1} [J]. Journal of Iron and Steel Research, International, 2015, 22(2):179-184.

[9] ZHANG W J, HAO P F, LIU Y, et al. Determination of the dynamic response of q345 steel materials by using SHPB [J]. Procedia Engineering, 2011, 24:773-777.

[10] TANG D W, WANG C Y, HU Y N, et al. Constitutive equation for hardened SKD11 steel at high temperature and high strain rate using the SHPB technique [J]. Proc-Spie, 2009, 7522: 75226B-75226B-12.

[11] QIN Z. High speed milling of hardened steel for dies and molds [D]. Guangzhou: Guangdong University of Technology, 2009. (in Chinese)

[12] JOHNSON G R, COOK W H. A constructive model and data for metals subjected to large strain, high strain rates and high temperature [C]// Proc 7th Int Symp on Ballistics. The Hague, Netherlands: American Defense Preparedness Association, 1983: 541-543.

[13] LI G H, WANG M J, KANG R K. Dynamic mechanical properties and constitutive model of Fe-36Ni invar alloy at high temperature and high strain rate [J]. Materials Science & Technology, 2010, 18: 824-829. (in Chinese)

[14] LI L, HE N, HE N. Experimental research on influence factors of cutting force and surface quality during high speed milling Al-alloy [J]. Tool Engineering, 2002, 36: 16-19. (in Chinese)

[15] WANG C Y, XIE Y X, ZHENG L J, et al. Research on the chip formation mechanism during the high-speed milling of hardened steel [J]. International Journal of Machine Tools & Manufacture, 2014, 79: 31-48.

Mr. **Ding Feng** is currently a Ph. D candidate at Guangdong University of Technology. His research interests cover high-speed machining for difficult-to-cut material and dynamic mechanical behaviors for metal.

Mr. **Tang Dewen** is currently a Ph. D candidate at Guangdong University of Technology. His research interests cover high-speed machining theory and numerical simulation technology.

Prof. **Wang Chengyong** is currently a professor at Guangdong University of Technology. His research interests cover high-speed machining for difficult-to-cut material, design and manufacture of medical devices and biological tissue resection theory.

Prof. **Zhang Fenglin** is currently a professor at Guangdong University of Technology. His research interest cover superhard cutting tools manufacturing and application technology.

Dr. **Zheng Lijuan** is currently an associate professor at Guangdong University of Technology. Her research interests cover printed circuit boards machining theory and cutting tool.

(Executive Editor: Zhang Tong)